Discrimination of Five Citrus Diseased Leaves by FTIR Spectroscopy

Xingxiang ZHAO, **Gang LIU** *, **Weixing LI**, **Xiaohua Wang**, **Jianming HAO**, **Xiangping ZHOU**

School of Physics and Electronic Information, Yunnan Normal University, Kunming 650500, China

Abstract　In this paper, citrus brown spot, huanglongbing, canker, fuliginous, *Cercospora* sp. and healthy leaves were studied using Fourier transform infrared spectroscopy (FTIR) combined with statistical analysis. The results showed that the spectra of the samples were similar, whereas there were obvious differences in the second derivatives of infrared spectra in the range of $1\ 500 - 700\ cm^{-1}$. The correlative analysis were evaluated, results showed that the correlation coefficients were larger than 0.918 between healthy leaves, and between the same diseased leaves. However, the values were all decreased between healthy and diseased leaves, and among different diseased leaves. The preprocessed original, first derivative and second derivative spectra in the range of $1\ 200 - 700\ cm^{-1}$ were chosen to evaluated principal component analysis (PCA) and hierarchical cluster analysis (HCA), respectively. The performance of the overall accuracy of PCA was 92.5%, which were better than original dataset and first derivative dataset. HCA by selecting second derivative dataset yield about 90% accuracy. This study proved that FTIR spectroscopy could be detected citrus diseases quickly and accurately.

Key words　FTIR, Citrus diseases, Principal component analysis, Cluster analysis

Citrus is belonging to *Rutaceae* family, which originates from a mutation of C. *Aurantieae*. Citrus is one of the major fruit products in the word. Citrus are suitable for planting in sunshine and rainfall areas in Asia, Africa and America. Flavonoid extracted from citrus fruits has been used in medicine and show many biological properties such as anti-viral, anti-cancer, anti-inflammatory, anti-atherogenicity and anti-thrombotic[1]. However, the quantity and quality of fruit are affected by diseases during growing and after harvest, and the benefits of farmers are also influenced by the diseases. Moreover, many diseases can not be prevented and controlled so far[2]. In fact, because the pathogens can not be detected rapidly and accurately, improper prevention methods and abusing chemicals not only pollute the environment but also go against the purpose of green, efficient and precision agriculture. Therefore, detection of citrus diseases correctly is very important to citrus production and customer. Serology, optical microscope and electron microscope have been used to detect citrus diseases, but these techniques have to go through series complex processes. In recent years, molecular techniques of citrus detection are polymerase chain reaction (PCR) based on specific deoxyribose nucleic acid (DNA) sequences of the pathogen, and enzyme-linked immunosorbent assay (ELISA) based on proteins produced by the pathogen. The limitations of the molecular techniques are time-consuming, labor-intensive and elaborate[3-4]. In recent years, spectroscopic and imaging techniques have been used to monitor citrus diseases with the advantage of speediness, accuracy and reliability. Fluorescence spectroscopy was employed to detect citrus disease stress caused by canker[5]. Qin et al. [6] employed hyperspectral reflectance imaging combined with PCA to detect citrus canker. Visible-near infrared and thermal imaging techniques were selected to detect citrus huanglongbing[7]. The near infrared spectral technology exhibit a more merit on the aspect of citrus disease non-destructive detection. FTIR has become one of the most useful techniques applied in biochemistry for studying the second structure of protein, carbohydrates and lipids. FTIR spectroscopy is a practical tool for a large-scale, real-time disease monitoring under field conditions. Cardinali et al. [8] employed FTIR spectroscopy combined with partial least square regression (PLS) to distinguish citrus variegated chlorosis and huanglongbing. Mid-infrared (MIR) spectroscopy combined with quadratic discriminant analysis (QDA) and k-nearest neighbor (kNN) were also applied to identify huanglongbing and healthy citrus leaves[9]. Hawkins et al. [10] compared FTIR spectral differences between citrus huanglongbing and other diseases. Fan reported that carbohydrate levels in huanglongbing-infected leaves with symptoms increased 7.9-fold compared to healthy controls[11]. Above reports focused on the discriminant analysis of citrus huanglongbing leaves. There were less reports using FTIR spectroscopy to detect citrus brown spot, canker, fuliginous and *Cercospora* sp. leaves.

In this paper, citrus brown spot, huanglongbing, canker, fuliginous, *Cercospora* sp. and healthy leaves were studied using FTIR combined with unsupervised pattern recognition. Huanglongbing and canker were caused by bacteria, brown spot, fuliginous and *Cercospora* sp. were caused by fungus.

1　Materials and methods

1.1　Samples　Brown spot, huanglongbing, canker, fuliginous, *Cercospora* sp. and healthy Leaves were collected from citrus ponkan in Yunnan of China. All infected trees considered had typical symptoms and were identified by qualified inspectors. The spot of diseased leaves and the corresponding part of health leaves was used for analysis. After grinding, the dried leaf powder was mixed with KBr and compressed into disc.

1.2　FTIR measurement　Fourier transform infrared spectra

were recorded on solid samples in KBr pellet form by means of a Tensor27 FTIR spectrometer (Bruker, Germany) equipped with a deuterated triglycine sulfide (DTGS) detector in the region of $4000 - 400$ cm^{-1}. The FTIR measurements were recorded in transmission mode. Data collection was acquired with a 4 cm^{-1} spectral resolution and 16 scans were accumulated each sample. A total of 40 spectra were collected.

1.3   Dataset treatment   To standardize data and reduce noise, the following operations were carried out: automatic baseline correction; normalization to the value 1.0 in relation to the most intensive band. To increase the resolution of obtained spectra, first derivatives and second derivatives (Savitzky − Golay algorithm, 5-point smoothing) were calculated. All operations on spectra were performed using original Omnic8.0 software and saved in CSV format, compatible with statistical software. Unsupervised multivariate statistical methods (HCA and PCA) were applied using the statistical packages of the SPSS16.0 software environment.
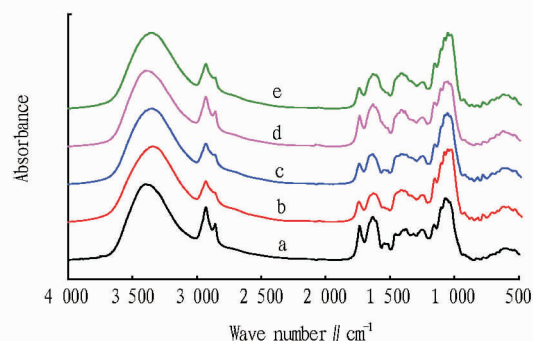
2   Results and analysis

2.1   Spectral characteristics of citrus leaves   Fig. 1 showed the infrared spectra of citrus brown spot, huanglongbing, canker, fuliginous, *Cercospora* sp. and healthy leaves. As can be seen from the figure, their spectra are similar representing some functional groups of lipids and carbohydrates. The strongest broad band at about 3 400 cm^{-1} was attributed to O − H stretching and contribution of N − H stretching[12]. The absorption bands in the $3\,000 - 2\,848$ cm^{-1} range were those assigned to asymmetric and symmetric methyl and methylene, the CH2 asymmetric stretching mode was positioned at around 2 917 cm^{-1}, while its symmetric stretching mode was positioned at about 2 850 cm^{-1}[13]. The absorption band around 1 735 cm^{-1} was correspond to C = O stretching vibration that mainly come from lipids. The mixed vibration absorption of cellulose, hemicellulose and lignin could be found clearly in the $1\,700 - 1\,500$ cm^{-1} range. The band around 1 610 cm^{-1} was assigned to the C = O stretching vibration of lignin[14].

The absorption bands in the $1\,500 - 1\,200$ cm^{-1} region was that assigned to the overlapped vibration absorption of fatty acids and polysaccharide[10−11]. The absorption band around 1 424 cm^{-1} was assigned to the CH group from scissoring vibration. The peaks in the range of $1\,440 - 1\,317$ cm^{-1} mainly came from CH3 and CH2 symmetric bending vibration absorption in cellulose and lignin affected by oxygen and nitrogen atoms[14−15]. The absorption bands in the $1\,200 - 700$ cm^{-1} region were contribution of polysaccharide and carbohydrate isomers, the peaks near 1 104 and 1 037 cm^{-1} were C − O and C − C stretching vibration of carbohydrate (cellulose and hemicellulose). Moreover, strong and broad absorption bands at 1 148, 1 105 and 1 037 cm^{-1} were mainly from the contribution of C = O stretching vibration in cellulose. Moreover, the absorption intensity was stronger gradually. It was showed that the main constitution of citrus leaves was lipids, lignin and polysaccharide.

There were observed tiny differences between diseased and healthy spectra. The absorption peak of lignin of *Cercospora* sp. was at 1 610 cm^{-1}, the other samples were shift to lower wave number at 1 606 cm^{-1}. The absorption bands of fuliginous observed at 2 926 and 2 850 cm^{-1} was stronger than others. The band of healthy leaves at 1 516 cm^{-1} was broad shoulder peak, while others were sharp peak. The strongest absorption intensity of polysaccharide contribution of huanglongbing and healthy leaves were positioned at 1 047, 1 037 cm^{-1}, respectively. The absorption ratio A1047/A2917 of all huanglongbing samples were larger than 1.423, but the values of all healthy samples were less than 1.173, it suggested that huanglongbing leaves accumulated more carbohydrate than healthy leaves. The result agreed with the study of Fan et al.[11]. The ratio A1047/A2917 might be as a marker for detecting huanglongbing.
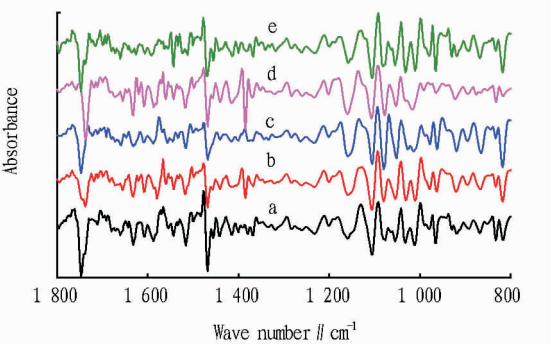

Note: a. Healthy; b. Brown Spot; c. Huanglongbing; d. Canker; e. Fuliginous; f. : *Cercospora* sp.

Fig. 1   FTIR spectra of healthy and diseased leaves in the range of 4000 − 400 cm^{-1}

2.2   The differences of second derivative spectra   For a good differentiation of the bands, the second derivative of the spectra was made. Commonly, the second derivatives of infrared spectra can obviously enhance the apparent resolution and amplify small differences in the infrared spectra. These were obtained with the Savitzky − Golay method (second-order polynomial with seven data points) using the Omnic8.0 software. The second derivative spectra of the samples were shown in Fig. 2. Some common absorption bands were found at 1 740, 1 515, and 1 231 cm^{-1}. From the second derivative FTIR spectra, several differences could be observed. The absorption bands of healthy sample at 1 175, 1 032, 922 cm^{-1} were stronger than that of the diseased samples. The intensity of the bands at 1 452, 1 392 and 1 231 cm^{-1} in brown spot, huanglongbing and canker samples increased comparison to healthy sample, while that of fuliginous and ercospora sp. samples decreased comparison to healthy sample. The band of healthy sample at 1031 cm^{-1} was strong and sharp, but in diseased sample appeared as broad bands. The absorption peak at 1018 cm^{-1} was found only in brown spot sample, while the others were at 1 032 and 1 013 cm^{-1}. Absorption bands of all samples at 922 cm^{-1} were strong except *Cercospora* sp sample.

2.3   Correlation analysis   The dataset in the second derivative spectrum in the range of $1\,200 - 700$ cm^{-1} were selected to evalu-
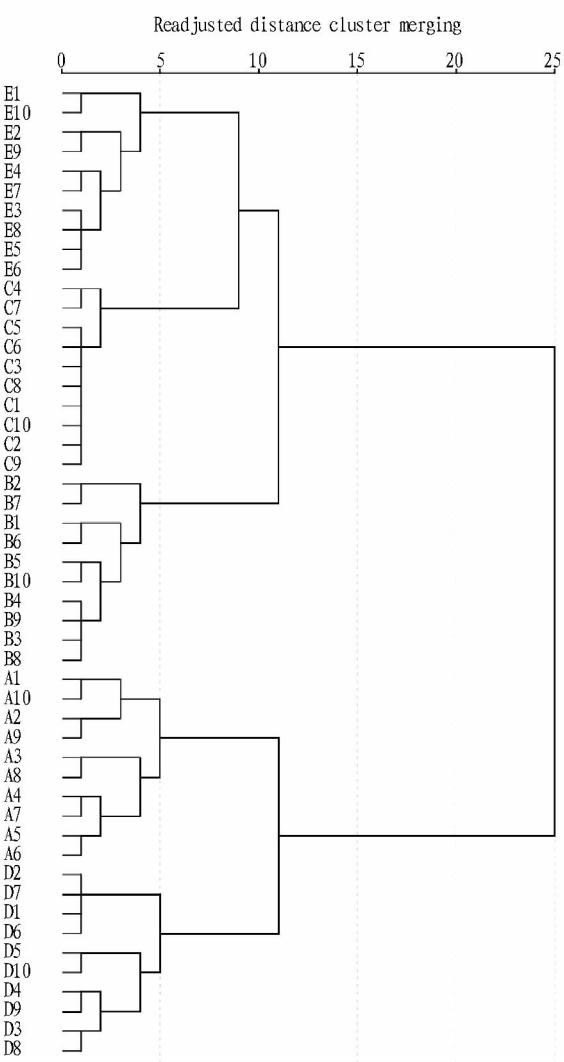
Note: a. Healthy; b. Brown Spot; c. Huanglongbing; d. Canker; e. Fuliginous; f. *Cercospora* sp.

Fig. 1 Second derivative spectra of healthy and diseased leaves in the range of 1 500 − 700 cm⁻¹

ate correlation coefficients. The results showed that the correlation coefficients were larger than 0. 928 not only between the healthy leaves, but also between the same diseased leaves. However, correlation coefficients of different diseased leaves and healthy leaves were different. The correlation coefficients of brown spot and healthy leaves ranged from 0. 650 to 0. 885, while the values of huanglongbing and healthy leaves ranged from 0. 850 to 0. 915, the correlation coefficients of brown spot, canker and healthy leaves ranged from 0. 661 to 0. 818. By comparison, the correlation degree between fuliginous and healthy leaves was the lowest, which ranged only from 0. 476 to 0. 564. The correlation coefficients exhibited differences among different kinds of diseased leaves, which suggested that the biotic stress factor had changed the chemical composition or the relative content of each component in citrus leaves.

2. 4 Principal Component Analysis Principal Component Analysis (PCA) is an unsupervised pattern recognition and is often the first step of exploratory data analysis to detect groups in the measured data. PCA models the directions of maximum variations in a data set by projecting as a swarm of points in a space defined by principal components (PCs). The performance of the overall accuracy of PCA on original and first derivative dataset was 60%, 87.5%, respectively. Fig. 3 showed the PCA performed on the second derivative spectra in the range of 1 200 − 700 cm⁻¹ of all samples that constituted six perfectly distinct groups. The score plots were projected in three-dimensional space. The first three PCs explained respectively 80%, 8% and 4% of the spectral variance. In the light of this PCA overview (92% of the spectral variance was explained with only 3 PCs), a good classification of citrus leaves was expected. The samples belonging to brown spot, huanglongbing, canker, fuliginous, and *Cercospora* sp groups were very close to each other, while the healthy samples had a large dispersion. As a whole, PCA results showed that the highest differentiation was between *Cercospora* sp and healthy leaves, the lowest between canker and huanglongbing. As seen from Fig. 3, all samples were classified into six groups with 92. 5% accuracy.

2. 5 Cluster analysis Cluster analysis was performed using Pearson's product moment correlation coefficient as a measure of
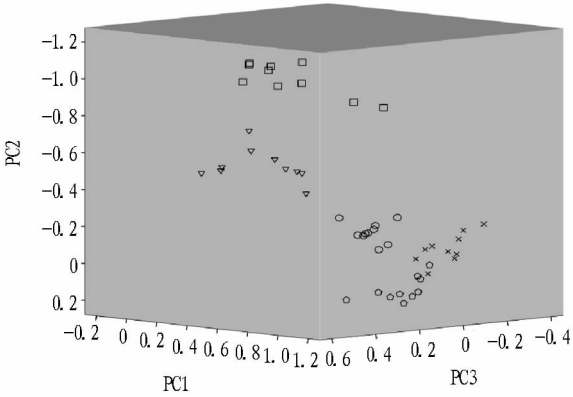

Note: ○. Healthy; +. Brown Spot; △. Huanglongbing; ◇. Danker; *. Fuliginous; ♀. *Cercospora* sp.

Fig. 3 PCA scores plots of healthy and diseased leaves on the second derivative spectra in the range of 1 200 − 700 cm⁻¹

similarity between the spectra, and Ward's algorithm to draw the dendrogram. Cluster analysis turned out to be a very useful tool for differentiating citrus diseases, as it revealed relationships among their FTIR spectra. Cluster analysis was evaluated in the first and second derivatives spectra respectively in 1 200 − 700 cm⁻¹ range. The results showed the accuracy of HCA by selecting the original and the first derivative dataset was 52. 5%, 80%, respectively. The best results were obtained in the case of the second derivative dataset (Fig. 4). Six major clusters were formed. Each of the citrus diseased and healthy leaves examined in the study formed a separate group. The shortest distances between spectra of citrus leaves were recorded within fuliginous and *Cercospora* sp, which indicate their highest similarity (highest homogeneity). These groups also showed the closest correlation. The most isolated clusters were formed by healthy leaves, which showed the lowest correlation with the other groups. However, b1, b3, c3 and a5 could

not be classified correctly belonging to their groups, the accuracy of HCA was 90%.

Note: a. Healthy; b. Brown Spot; c. Huanglongbing; d. Canker; e. Fuliginous; f. *Cercospora* sp.

Fig. 4 Dendrogram from hierarchical cluster analysis results of healthy and diseased leaves on the second derivative spectra in the range of 1 200 – 700 cm^{-1}

3 Conclusions

Citrus diseased and healthy leaves were explored using Fourier transform infrared spectroscopy combined with multivariate statistical analysis. The correlative coefficients of the second derivative dataset were obviously different, which showed biotic stress had changed the chemical composition and relative content of components. The citrus diseased and healthy leaves could be classified correctly using the principal component analysis and hierarchical cluster analysis by selecting the second derivative spectra in the region of 1 200 – 700 cm^{-1}. The results showed that FTIR technique was used to detect citrus diseases with rapid, non-destructive, feasible and accurate advantages. Future studies would involve the evaluation of this technique for detecting non-symptomatic citrus diseased leaves infected by microorganism. The ability of FTIR spectroscopy to show the changes in the chemistry of the plant before visible symptoms in many of the samples, along with its ease of use, speed, and relative cost, could lead to its increased use as a predictive method in the future.

References

[1] BARRECA D, BELLOCCO E, GATTUSO G, et al. Polyphenol composition, vitamin C content and antioxidant capacity of *Mauritian citrus* fruit pulps[J]. Food Chemistry, 2011(129): 1504 – 1512.

[2] EHSANI R, MISHRA A, SANKARAN S, et al. A review of advanced techniques for detecting plant diseases[J]. Computers and Electronics in Agriculture, 2010(72): 1 – 13.

[3] LI WB, LEVY L, HARTUNG JS. Quantitative distribution of 'Candidatus Liberibacter asiaticus' in citrus plants with citrus Huanglongbing[J]. Bacteriology, 2009(99): 139 – 144.

[4] TEIXEIRA DC, SAILLARD C, COUTURE C, et al. Distribution and quantification of Candidatus Liberibacter americanus, agent of huanglongbing disease of citrus in So Paulo State, Brasil, in leaves of an affected sweet orange tree as determined by PCR[J]. Molecular and Cellular Probes, 2008 (22): 139 – 150.

[5] LINS EC, BELASQUE JJ, MARCASSA LG. Detection of citrus canker in citrus plants using laser induced fluorescence spectroscopy[J]. Applied Optics, 2008(47): 1922 – 1926.

[6] QIN JW, BURKS TF, KIM MS, et al. Citrus canker detection using hyperspectral reflectance imaging and PCA-based image classification method[J]. Sensor and Instrument Food Quality, 2008(2): 168 – 177.

[7] SANKARAN S, MAJA JM, BUCHANON S, et al. Huanglongbing (citrus greening) detection using visible, near Infrared and Thermal Imaging Techniques, Sensors, 2013(13): 2117 – 2130.

[8] CARDINALI MCDB, BOASA PRV, MILORI DMBP, et al. Infrared spectroscopy: A potential tool in huanglongbing and citrus variegated chlorosis diagnosis[J]. Talanta, 2012(91): 1 – 6.

[9] SANKARAN S, EHSANI R, ETXEBERRIA E. Mid-infrared spectroscopy for detection of Huanglongbing (greening) in citrus leaves[J]. Talanta, 2010(83): 574 – 581.

[10] HAWKINS SA, PARK B, POOLE GH, et al. Comparison of FTIR spectra between Huanglongbing (*Citrus greening*) and other citrus maladies[J]. Journal of Agriculture and Food Chemistry, 2010(58): 6007 – 6010.

[11] FAN J, CHEN C, BRLANSKY RH, et al. Changes in carbohydrate metabolism in *Citrus sinensis* infected with 'Candidatus Liberibacter asiaticus' [J]. Plant Pathology, 2010(59): 1037 – 1043.

[12] GORGULU ST, DOGAN M, SEVERAN F. The Characterization and Differentiation of Higher Plants by Fourier Transform Infrared Spectroscopy [J]. Applied Spectroscopy, 2007(61): 300 – 308.

[13] MONTI F, ANNA RD, SANSON A, et al. A multivariate statistical analysis approach to highlight molecular processes in plant cell walls through ATR FT-IR microspectroscopy: The role of the α-expansin PhEXPA1 in Petunia hybrida[J]. Vibrational Spectroscopy, 2013(65): 36 – 43.

[14] ALLISONll GG, MORRIKS C, HODGSON E, et al. Measurement of key compositional parameters in two species of energy grass by Fourier transform infrared spectroscopy[J]. Bioresource Technology, 2009(100): 6428 – 6433.

[15] YANG HP, YAN R, CHEN HP, et al. Characteristics of hemicellulose, cellulose and lignin pyrolysis[J]. Fuel, 2007(86): 1781 – 1788.

◇◆

of all expired foods into the database. Supervision department shall examine data in the database, check information of expired foods in time, and supervise enterprises to strictly manage expired foods in accordance with regulations. More important, food production and processing enterprises and sellers should not treat expired foods on their own, but send expired foods to a special food recovery department or the third party authorized by the State, to increase efficiency in recovery processing of expired foods, and effectively avoid reverse flow of expired foods. Food recovery department and the third party recovery enterprises shall check the database, feedback treatment of expired foods in time, classify and test expired foods, and recycle expired foods in accordance with their properties, to avoid waste and reduce eco-

nomic losses to the maximum extent.

References

[1] DU ZX. Analysis on reclamation and destruction system of expired food[J]. Legal & Economy, 2009(12): 125 – 126. (in Chinese).

[2] FANG QA, YAO QH. Constructing centralized handling mechanism for unsafe food, improving comprehensive effectiveness of food circulation safety [J]. Study on China Administration for Industry & Commerce, 2010(10): 32 – 34. (in Chinese).

[3] WANG K, NAN Y. A brief discussion on supervision of expired food[J]. China Brand and Anti-counterfeiting, 2011(12): 88 – 89. (in Chinese).

[4] LI XM, WANG Y. The institutional defect of never expired food and its governance[J]. China Business & Trade, 2012(5): 82. (in Chinese).

[5] YU ZY, YIN YG. Lessons from food safety management measures of foreign countries[J]. Marketing Research, 2011(6): 49 – 53. (in Chinese).